Nonlinear control of multicellular single stage grid connected photovoltaic systems with shunt active power filtering capability

Aourir, M.; Abouloifa, A.; Aouadi, C.; El Otmani, F.; Lachkar, I.; Giri, F.; Guerrero, Josep M.

Published in:
IFAC-PapersOnLine

DOI (link to publication from Publisher):
10.1016/j.ifacol.2020.12.2091

Publication date:
2020

Document Version
Publisher's PDF, also known as Version of record

Available online at www.sciencedirect.com

ScienceDirect

IFAC PapersOnLine 53-2 (2020) 12853–12858

Nonlinear Control of Multicellular Single Stage Grid Connected Photovoltaic Systems with Shunt Active Power Filtering Capability

M. Aourir * **A. Abouloifa** * **C. Aouadi** * **F. EL Otmani** *
I. Lachkar ** **F. Giri** *** **Josep M. Guerrero** ****

* *TI laboratory, Hassan II university, Bp 7955, Casablanca, Morocco (e-mail: meriem.aourir-etu@etu.univh2c.ma).*
** *ESE laboratory, ENSEM of casablanca, Hassan II university, Bp 8118, Casablanca, Morocco*
*** *Normandie UNIV, UNICAEN, ENSICAEN, LAC, 14000 Caen, France*
**** *Department of Energy Technology, AAU, 9220 Aalborg East, Denmark*

Abstract: This work deals with the nonlinear control of grid connected photovoltaic (PV) systems with shunt active power filtering functionality. The Proposed power plant consists of two PV generators, a single-phase power grid connected to non-linear loads at point of common coupling (PCC) and a multicellular inverter that will play a dual role, on one hand, compensating harmonic currents and reactive power caused by non-linear loads, and on the other hand, injecting active power provided by the PV generators into the electrical grid. The proposed nonlinear controller is designed in order to achieve the following objectives: i) guarantee a balanced distribution of the input voltage over the power switching devices, ii) ensure a unity power factor in the grid by compensating harmonic currents and reactive power, iii) operate the PV panels in their optimal operating points by extracting the maximum power despite the climatic variations. In order to achieve these objectives, a cascaded non-linear controller, consisting of two loops is designed, an outer loop based on a filtered PI controller for the regulation of PV panels voltages and, an inner loop developed based on Lyapunov approach for power factor correction as well as flying capacitors voltages regulation. Furthermore, a state observer is combined with the non-linear controller to perform the grid voltage estimation. The proposed power plant and control strategies are verified and validated by numerical simulation using Matlab/SimPowerSystems environment to assess their performance.

Keywords: PV systems, Shunt active power filter, Power factor correction, state observer, Lyapunov approach, MPPT.

1. INTRODUCTION

Presently, PV solar energy is seen as the most commonly used renewable energy sources, since it is inexhaustible, environmentally harmless and, especially, the cost-effectiveness is guaranteed. However, the maximum power of PV modules is strongly influenced by the irradiance and temperature, therefore, tracking the maximal power point in any climatic condition is required. In literature, different algorithms and techniques for maximal power point tracking (MPPT) have been proposed (Karami et al. (2017)), such as perturb & observe (P&O), Fuzzy logic, incremental conductance (IncCond) and, so on. The incremental conductance algorithm has been selected for this work due to its adaptability to rapid changes in climate conditions, as well as its ease of implementation since a minimal knowledge about the PV system is needed (Putri et al. (2015)).

The high emergence of photovoltaic power plants has been matched by the implementation of various grid-connected PV system architectures, where, the power matching stages are used to increase the system reliability and efficiency. Two types of grid connected PV topologies can be identified, the double stage PV systems and single stage ones (see Jana et al. (2017)), in the former, DC/DC and DC/AC converters are used to transmit the produced energy from the PV modules to the utility grid, where in the latter, DC/AC converters are only used to deal with the PV system requirements.

Single stage grid connected PV systems have the advantage of using minimum power switching devices which reduces losses and increases system reliability. Nevertheless, a high power rate of PV panels is needed, which increases the voltage stress on the power switching devices. To face this challenge, multilevel converters have been used as they can operate at high voltage levels by adopting low voltage rated power switching devices. In such kind of inverters, improved output waveforms with lower total

10.1016/j.ifacol.2020.12.2091

harmonic distortion (THD) are further offered (Rodriguez et al. (2007)).

As the use of non-linear loads expands, the energy quality tends to deteriorate. Moreover, it is well known that electronic power equipment constitutes the major part of the non-linear loads that lead to the generation of higher order harmonics and the consumption of reactive power (Abouloifa et al. (2014)). As a result, shunt active power filters (SAPF) have been the most suitable solution for harmonic currents and reactive power compensation due to their flexibility and high filtering ability.

The control problem of grid connected PV systems and SAPFs has attracted a great deal of attention from researchers. In this light, various control approaches have been proposed to enhance the system dynamics and efficiency. Generally, linear methods and nonlinear ones can be identified. In this respect, in Abo-Elyousr and Abdelaziz (2018) the authors have proposed an optimal proportional integral (PI) regulator for single stage-based H-bridge inverter for PV grid-tied systems, the effectiveness of the proposed controller was verified by numerical simulations and experimental implementation. A more sophisticated PI controller has been proposed in Sefa et al. (2015), where the PI parameters are tuned using fuzzy logic controller which permits to take into account different operation conditions in grid-tied PV systems. On the other side, backstepping nonlinear controller has been proposed in Aourir et al. (2017) for PV grid connected systems, the performance of the proposed controller was verified by numerical simulations. Additionally, a sliding mode approach has been proposed in (Aouadi et al. (2016)), where, fast dynamic response and strong robustness have been proved. For more accurate harmonic currents and reactive power compensation, several control strategies have been developed for SAPFs. In Lada et al. (2016), the authors have suggested instantaneous power theory for single-phase cascaded multilevel inverter, the results show good performance in term of harmonic currents and reactive power compensation. Finally, an improved tracking strategy using sliding mode and feedback linearization has been proposed in Sinha Ray and Bhattacharya (2016).

In this work, single stage grid connected PV system based on multicellular inverter with active filtering capability in presence of non-linear loads has been considered. The studied power plant addresses the problem of power enhancement in the single stage structures as well as the problem of distorted power quality caused by non-linear loads.

This paper is organized as follows. In section 2, the suggested system consisting of PV generators associated to SAPF is described and modelled. Then, the structure of the proposed controller and state observer design is presented in section 3. To assess the effectiveness of the suggested power plant and controller combined with the state observer, numerical simulation results are given and discussed in section 4. Conclusion and a list of references are finally presented.

2. STUDIED SYSTEM DESCRIPTION AND MODELLING

The configuration of the proposed power plant depicted in Fig. 1 consists of two identical PV generators, capacitive

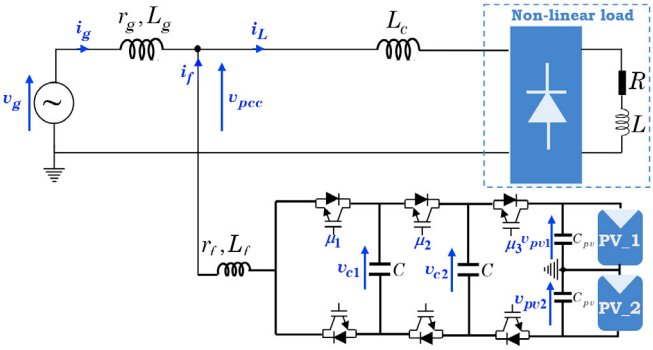

Fig. 1. Proposed SAPF with active power injection

divider of energy storage C_{pv}, multilevel inverter with IGBT-diode as switching devices and an output L-filter. This assembly is connected at the point of common coupling (PCC) to a single-phase power grid and a nonlinear load formed by diode-bridge rectifier feeding RL inductive load.

The used multicellular inverter for active power injection in the grid, harmonic currents and reactive power compensation consists of three imbricated cells where each one is controlled in complementary way (i.e. if the upper switch is ON, the lower is OFF). This topology has the advantage of reducing the voltage stress dv/dt on the power switching devices, which is very attractive in the case of a high input power that is considered in this work. Besides, this topology offers lower harmonics in the output waveforms, which leads to the use of smaller size filter components.

To ensure the normal operation of the multicellular inverter with n-cell, it is necessary that the voltage rating in the flying capacitors has the following distribution:

$$v_{ck} = k\frac{(v_{pv1} + v_{pv2})}{n} \text{ for } k \in \{1, ..., n-1\} \tag{1}$$

This guarantees a balanced distribution of the input voltage on the power switching devices, therefore, under equilibrium condition each cell will take the same value given by:

$$v_{cell} = \frac{v_{pv1} + v_{pv2}}{n} \tag{2}$$

By applying Kirchhoff's laws to the system presented in Fig. 1, the following switched model is obtained:

$$C\frac{dv_{c1}}{dt} = (\mu_2 - \mu_1)i_f \tag{3a}$$

$$C\frac{dv_{c2}}{dt} = (\mu_3 - \mu_2)i_f \tag{3b}$$

$$\begin{aligned} L_f\frac{di_f}{dt} =& (\mu_1 - \mu_2)v_{c1} + (\mu_2 - \mu_3)v_{c2} + \mu_3(v_{pv1} + v_{pv2}) \\ & - r_f i_f - v_{pv2} - v_{pcc} \end{aligned} \tag{3c}$$

$$C_{pv}\frac{dv_{pv1}}{dt} = i_{pv1} - \mu_3 i_f \tag{3d}$$

$$C_{pv}\frac{dv_{pv2}}{dt} = i_{pv2} + (1 - \mu_3)i_f \tag{3e}$$

$$L_g\frac{di_g}{dt} = v_g - v_{pcc} - r_g i_g \tag{3f}$$

On account of the binary nature of the control signals μ_1, μ_2 and μ_3, the model (3) cannot be used for the

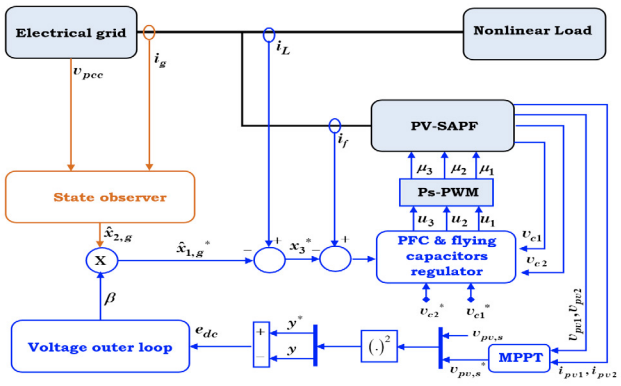

Fig. 2. Controlled PV system

development of continuous control laws. Therefore, we resorted to the following average model:

$$C\frac{dx_1}{dt} = (u_2 - u_1)x_3 \tag{4a}$$

$$C\frac{dx_2}{dt} = (u_3 - u_2)x_3 \tag{4b}$$

$$L_f\frac{dx_3}{dt} = (u_1 - u_2)x_1 + (u_2 - u_3)x_2 + u_3x_4 - r_fx_3 - \frac{x_4}{2} - v_{pcc} \tag{4c}$$

$$C_{pv}\frac{dx_4}{dt} = i_{pv1} + i_{pv2} - (1 - 2u_3)x_3 \tag{4d}$$

$$L_g\frac{dx_{1,g}}{dt} = x_{2,g} - v_{pcc} - r_gx_{1,g} \tag{4e}$$

The state variables $x_1, x_2, x_3, x_4, x_{1,g}$ and the input signals u_1, u_2, u_3 are respectively the average values over cutting period of the state variables $v_{c1}, v_{c2}, i_f, v_{pv1} + v_{pv2}, i_g$ and the binary input signals μ_1, μ_2, μ_3.
Equation (4e) is completed with the following internal states of the electrical grid:

$$\frac{dx_{2,g}}{dt} = x_{3,g} \tag{5a}$$

$$\frac{dx_{3,g}}{dt} = -\omega_g^2x_{2,g} \tag{5b}$$

where $x_{2,g} = v_g$ and $x_{3,g} = \dot{v}_g$.

3. NONLINEAR CONTROLLER AND STATE OBSERVER DESIGN

In this section, the designed multi-loop nonlinear controller of the SAPF based on multicellular inverter with PV power injection into the grid will be presented. The proposed control strategy has to fulfil the following objectives: i) ensure the power factor correction, ii) compensate harmonic currents and reactive power, iii) guarantee an equitable distribution of the input voltage at the power switching devices, iv) extract the maximum amount of power from the PV panels (MPPT task).
As illustrated in Fig. 2, the controller layout is formed by two cascaded loops. On one side, the outer loop for the PV panels voltage regulation made by a PI regulator that compares the PV panels voltage reference provided by the MPPT block to the actual measured PV panels voltage. On the other side, the inner loop is used to concurrently perform power factor correction and regulation of flying capacitor voltages.

3.1 Inner loop: Power factor correction and Regulation of flying capacitor voltages

Regulation of flying capacitor voltages The main purpose is to ensure the safe operation of the multicellular inverter which consists of obtaining an equilibrated distribution of the input voltage at the different power switching devices ($v_{pvs}/3$), therefore the regulation of the voltage across the flying capacitors is needed.

In this respect, one introduces the following tracking error vector associated to flying capacitors voltage:

$$Z = \begin{pmatrix} z_1 \\ z_2 \end{pmatrix} = C\begin{pmatrix} x_1 - x_1^* \\ x_2 - x_2^* \end{pmatrix} \tag{6}$$

Using (4a-b), the time derivative of (6) is then obtained.

$$\dot{Z} = \begin{pmatrix} \dot{z_1} \\ \dot{z_2} \end{pmatrix} = \begin{pmatrix} \delta_1x_3 - C\dot{x}_1^* \\ \delta_2x_3 - C\dot{x}_2^* \end{pmatrix} \tag{7}$$

where $\delta_1 = u_2 - u_1$ and $\delta_2 = u_3 - u_2$ are the control inputs for the flying capacitors balancing.
From (7), it can be seen that the effective control inputs have appeared, then an appropriate control laws must be established in order to make the Z-system globally asymptotically stable. To this end, the following Lyapunov function candidate is considered

$$V = 0.5z_1^2 + 0.5z_2^2 \tag{8}$$

Using (7), it is deduced that the dynamic of Lyapunov function candidate along the trajectory of Z is

$$\dot{V} = (\delta_1x_3 - C\dot{x}_1^*)z_1 + (\delta_2x_3 - C\dot{x}_2^*)z_2 \tag{9}$$

To make $\dot{V}$ negative definite function, the following choice will be enforced

$$\begin{cases} \delta_1x_3 - C\dot{x}_1^* = -c_1z_1 \\ \delta_2x_3 - C\dot{x}_2^* = -c_2z_2 \end{cases} \tag{10}$$

where c_1 and c_2 are real positive design parameters.
The actual control laws are derived from the above equation and are given by:

$$\begin{pmatrix} \delta_1 \\ \delta_2 \end{pmatrix} = \frac{1}{x_3}\begin{pmatrix} -c_1z_1 + C\dot{x}_1^* \\ -c_2z_2 + C\dot{x}_2^* \end{pmatrix}. \tag{11}$$

Power factor correction Prior to proceed with the design of the control law ensuring harmonic currents and reactive power compensation with PV power injection into the grid, a state observer is first designed to estimate the grid voltage.
It is obvious to establish that (4e) and (5) are expressed in the following compact form

$$\begin{cases} \dot{X}_g = AX_g + B \\ Y_g = CX_g \end{cases} \tag{12}$$

with $X_g = \begin{pmatrix} x_{1,g} \\ x_{2,g} \\ x_{3,g} \end{pmatrix}$, $A = \begin{pmatrix} -r_g/L_g & 1/L_g & 0 \\ 0 & 0 & 1 \\ 0 & -\omega_g^2 & 0 \end{pmatrix}$,
$B = \begin{pmatrix} -v_{pcc}/L_g \\ 0 \\ 0 \end{pmatrix}$ and $C^T = \begin{pmatrix} 1 \\ 0 \\ 0 \end{pmatrix}$
Then, the following state observer is employed:

$$\dot{\widehat{X}}_g = A\widehat{X}_g + B + \rho(y_g - C\widehat{y}_g) \tag{13}$$

where ρ is the observer's gain $\rho = (\rho_1\ \rho_2\ \rho_3)^T$ and the conditions on it will be introduced thereafter. Now, in

order to analyze the observer, the following observer error has been used

$$\widetilde{X}_g = \widehat{X}_g - X_g \tag{14}$$

Using (12) and (13), it results that the estimation error undergoes the following expression:

$$\dot{\widetilde{X}}_g = (A - \rho C)\widetilde{X}_g \tag{15}$$

The gain of the state observer must be chosen so that the eigenvalues of $(A-\rho C)$ have negative real parts. Therefore, by applying Routh-Hurwitz criteria, it follows that:

$$\frac{r_g}{L_g} + \rho_1 > 0, \frac{r_g}{L_g} + \rho_1 > -\frac{\rho_3}{L_g\omega^2} \text{ and } \frac{r_g}{L_g} + \rho_1 > \frac{\rho_3}{\rho_2}$$

Currently, the main purpose is to simultaneously, compensate harmonic currents and reactive power caused by nonlinear loads, and inject the remaining amount of PV power into the electrical grid with a unity power factor. To serve this end, the filter output current is forced to follow its reference $x_3^* = i_L - \beta\hat{x}_{2,g}$ according to the operating mode (i.e. active filter only, active filtering with PV power injection into the power grid simultaneously or PV power injection into the power grid only). In this respect, the following current tracking error is defined:

$$z_3 = L_f(x_3 - x_3^*) \tag{16}$$

Using (4c) and (13), the time derivative of (16) is:

$$\begin{aligned} \dot{z_3} = &-\delta_1 x_1 - \delta_2 x_2 + u_3 x_4 - 0.5x_4 - r_f x_3 - v_{pcc} \\ &-L_f(\frac{di_L}{dt} - \beta(\dot{\hat{x}}_{3,g} - \rho_2\tilde{x}_{1,g}) - \dot{\beta}\hat{x}_{2,g}) \end{aligned} \tag{17}$$

From the above equation, it can be seen that the actual control input u_3 has appeared, consequently, to make the z_3-system asymptotically stable with respect to the Lyapunov function candidate $V_2 = 0.5z_3^2$, it is sufficient to choose the control input u_3 so that $\dot{V}_2 = \dot{z_3}z_3$ be a negative definite function which yields to the following choice

$$\dot{z_3} = -c_3 z_3 \tag{18}$$

Comparing (17) and (18), and using (11) the following effective control input is given:

$$\begin{aligned} u_3 = &\frac{1}{x_4}[-c_3 z_3 + 0.5x_4 + r_f x_3 + v_{pcc} + (-c_1 z_1 + C\dot{x_1^*})\frac{x_1}{x_3} \\ &+(-c_2 z_2 + C\dot{x_2^*})\frac{x_2}{x_3} + L_f(\frac{di_L}{dt} - \beta(\hat{x}_{3,g} - \rho_2\tilde{x}_{1,g}) - \dot{\beta}\hat{x}_{2,g})] \end{aligned} \tag{19a}$$

Considering (11) and the above equation, the last two control inputs are then given as follows:

$$u_2 = u_3 - \frac{1}{x_3}(-c_2 z_2 - C\dot{x_2^*}) \tag{19b}$$

$$u_1 = u_2 - \frac{1}{x_3}(-c_1 z_1 - C\dot{x_1^*}) \tag{19c}$$

3.2 Outer loop: PV voltage regulation (MPPT issue)

The main focus of this part of control is to ensure the power balance between the PV generators, the nonlinear load and the electrical grid. For this purpose, the additional control law β introduced in (17) must be designed so that the squared voltage of PV generators $y = {x_4}^2$ is directed towards the reference value $y^* = (x_4^*)^2$ provided by the MPPT block. As a first step, the relationship between the squared voltage y and β is given and described in proposition 1 by considering the assumption of similarity of PV panels and a common climatic conditions exposition.

Proposition 1. Consider the investigated system shown in Fig. 1, described by the average model (4), and the internal control laws (19), therefore, the relationship between y and β is given by the following time varying equation:

$$\dot{y} = K + f_1(\beta, \dot{\beta}, Z, \widetilde{X}_g) + f_2(t, \beta, \dot{\beta}, Z, \widetilde{X}_g) \tag{20}$$

with

$$K = \frac{4P_{pv}}{C_f} - \frac{2r_f}{C_f}\sum_{h=1}^{\infty} {i_{L,h}}^2 - \frac{4E_g i_{L,1}}{C_f}\cos(\phi_1)$$

$$\begin{aligned} f_1(\beta, \dot{\beta}, Z, \widetilde{X}_g) = &-\frac{4}{C_f}(-c_1 z_1 x_1 - c_2 z_2 x_2) - \frac{4\beta\hat{x}_{2,g}}{C_f}[-c_3 z_3 \\ &+\beta r_f \hat{x}_{2,g} + \beta L_f \rho_2 \hat{x}_{1,g} + L_f\dot{\beta}\hat{x}_{2,g} + L_f\beta\dot{\hat{x}}_{2,g}] - \frac{4E_g^2 L_f}{Cf}\beta\dot{\beta} \\ &+\frac{2E_g i_{L,1}}{C_f}(2L_f\beta\omega\sin(\phi_1) - \cos(\phi_1)(2r_f\beta - r_g\beta - L_f\dot{\beta})) \end{aligned}$$

$$\begin{aligned} f_2(t, \beta, \dot{\beta}, Z, \widetilde{X}_g) = &-\frac{4}{C_f}\{(-c_3 z_3 - \beta\rho_2\tilde{x}_{1,g})(i_L - \beta x_{2,g}) \\ &+\rho_2 L_f \beta\tilde{x}_{2,g} i_L - L_f\frac{di_L}{dt}\beta(x_{2,g} + \tilde{x}_{2,g}) + z_3\left(c_3 + \frac{r_g}{L_f}\right)i_L \\ &-r_f\sum_{h=1}^{\infty}\frac{{i_{L,h}}^2}{2}\cos(2h\omega t + 2\varphi_h) + \beta x_{2,g}\tilde{x}_{2,g}(2r_f - \beta\rho_2 L_f) \\ &-\frac{{E_g}^2}{2}\cos(2\omega t)\beta\left(r_f + \dot{\beta}L_f\right) - \beta z_3\left(c_3 + \frac{r_g}{L_f}\right)x_{2,g} \\ &+L_f\frac{d^2 i_L}{dt} - \left(\beta r_g + L_f\dot{\beta}\right)(\tilde{x}_{2,g} i_L - \beta\tilde{x}_{2,g} x_{2,g}) \\ &+\frac{E_g i_{L,1}}{2}\cos(2\omega t + \varphi_1) - L_f\beta\frac{E_g\omega i_{L,1}}{2}\sin(2\omega t + \varphi_1) \\ &+\beta\frac{{E_g}^2}{2}\cos(2\omega t) - \frac{E_g i_{L,1}}{2}\sin(2\omega t)\cos(\varphi_1) \\ &-\sum_{h=2}^{\infty} i_{L,h}\sin(h\omega t + \varphi_h)\left(2\beta r_f + \dot{\beta}\right) + i_L\tilde{x}_{2,g}(\dot{\beta} - 2\beta r_f) \\ &-\cos(2\omega t)\left(\frac{L_f\dot{\beta}\beta{E_g}^2}{2} - \frac{E_g i_{L,1}}{2}\sin(\varphi_1)(1 - r_g\beta - L_f\dot{\beta})\right) \\ &+\left(1 - r_g\beta - L_f\dot{\beta} - 2r_f\beta\right)\sum_{h=2}^{\infty} i_{L,h}\sin(h\omega t + \varphi_h) \\ &+L_f\beta^2(x_{2,g}\dot{x}_{2,g} + \tilde{x}_{2,g}\dot{x}_{2,g} + x_{2,g}\rho_2\tilde{x}_{2,g}) \\ &-\beta\tilde{x}_{2,g} v_{pcc} + \beta^3 L_f\dot{x}_{2,g} x_{2,g} - \beta\dot{\beta}2x_{2,g}\tilde{x}_{2,g}\} \end{aligned}$$

Proof. Equation (20) is obtained by replacing the expressions of the control laws given by (19) into (4d), calculation details are omitted due to limited space constraints.

In the interest of ensuring the power balance between the PV generators, the nonlinear load and the power grid, the design of the tuning law for β with the premise that its first derivative must be available (proposition 1), the following filtered PI regulator is adopted:

$$\beta = \frac{1}{1 + \frac{1}{c_4}s}(k_p z_4 + k_i z_5) \tag{21}$$

where $z_4 = y^* - y$ and $z_5 = \int z_4 d\tau$

s denotes the Laplace variable and (c_4, k_p, k_i) are real positive design parameters. From (21), the first derivative of β is computed using the following equation:

Table 1. System Characteristics

Subsystems	Symbol	Values
Electrical grid	E_g, f_g	$220\sqrt{2}, 50Hz$
	r_g, L_g	$0.5m\Omega, 0.2mH$
Multicelluar shunt active power filter	C_{pv}	$6mF$
	C	$40\mu F$
	r_f, L_f	$5m\Omega, 3mH$
RL load	R, L	$10\Omega, 0.5H$
Switching frequency	f_s	$10kHz$
Inner loop regulator	c_1	$15.10^3 s^{-1}$
	c_2	$15.10^3 s^{-1}$
	c_3	$17.10^3 s^{-1}$
outer loop regulator	k_p	$1.95.10^{-5} V^{-2}\Omega^{-1}$
	k_i	$4.99.10^{-4} s^{-1} V^{-2}\Omega^{-1}$
	c_4	$200s^{-1}$
State observer	ρ_1	$5000s^{-1}$
	ρ_2	$500s^{-1}\Omega$
	ρ_3	$500s^{-2}\Omega$

$$\dot{\beta} = c_4(k_p z_4 + k_i z_5 - \beta) \tag{22}$$

4. SIMULATION RESULTS

The entire system, including the controller/state observer scheme, is simulated under MATLAB/SimpowerSystems environment to evaluate its performance. The corresponding parameters of the power plant and the designed controller and state observer are described in Table 1.

To assess the performance of the studied system, three operating modes have been considered:

- Operating mode 1: In this mode, a low PV power ($P_{pv} < P_L$) is available, in fact, the electrical network will supply the active power required by the non-linear load.
- Operating mode 2: In this mode, the PV generators provide their maximum power ($P_{pv} = 7kW$) corresponding to the standard climatic conditions (i.e. $\lambda = 1kW/m^2$ and $T = 25°C$), in this case, the PV generators supply the amount of active power required by the nonlinear load, while the remaining power ($P_{pv} - P_L$) will be injected into the power grid.
- Operating mode 3: in this mode, no load is associated with the power grid, therefore, the maximum PV power supplied by the PV generators will be fully injected into the power grid.

These operating modes are tested in a common simulation pattern described in Table 2.

Table 2. Simulation pattern description

Operating modes	Mode 1	Mode 2	Mode 3
Time span	$0 \rightarrow 0.5s$	$0.5 \rightarrow 1s$	$1 \rightarrow 1.4s$
PV power	$P_{pv} = 0.12kW$	$P_{pv} = 7kW$	$P_{pv} = 7kW$
Load power	$P_L = 3.77kW$	$P_L = 3.77kW$	$P_L = 0$

The obtained simulation results that corresponds to the step variation in irradiance from $0.02kW/m^2$ to $1kW/m^2$ at time $0.5s$ are shown in Fig. 3-10. Fig. 3 illustrates that in mode 1, the power grid provides the required active power by the non-linear load, while in mode 2, it can be seen that the maximum PV power is greater than the required load power, as a result, the remaining power is injected into the grid, for the last mode the maximum amount of the extracted PV power is totally injected into the grid. From Fig. 4, it can be seen that the PV panels voltage reaches its reference provided by the MPPT block according to the irradiance variation and thus the maximal PV panels power is extracted. Fig. 5 shows the flying capacitor voltages trajectories where they track their references and thus an equilibrated distribution of the input voltage at the power switching devices is then obtained. The filter output current waveform is shown in Fig. 6, one can see that the shape and the amplitude of this current change according to the operating mode. The performance of the designed state observer is demonstrated by Fig. 7 where it can be seen that the estimated grid voltage $\hat{x}_{2,g}$ converges rapidly to its true value $x_{2,g}$. The PFC objective is achieved with high efficiency as illustrated in Fig. 8, where the estimated grid current has a sinusoidal shape and in phase (or opposite) with the estimated grid voltage. The FFT analysis of non-linear load current indicates a THD of 41.75% (Fig. 9). Where, the grid current THD is about 2.44% (Fig. 10) which confirms that the grid current is actually sinusoidal. Further results of the obtained THD for the three operating modes are given in Table 3.

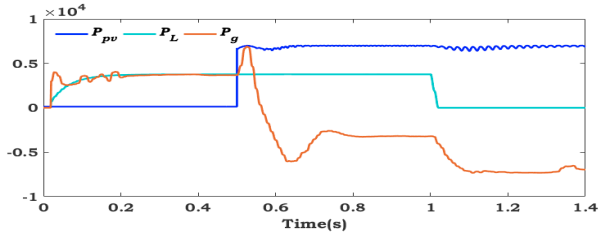

Fig. 3. Active power of the power grid, non-linear load and the power generated by PV panels

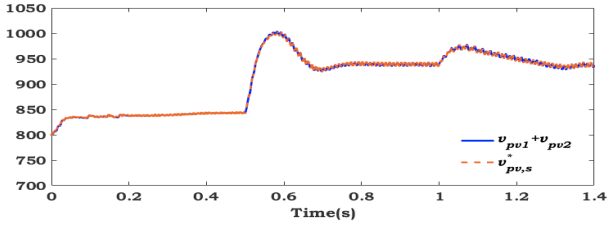

Fig. 4. PV panels voltage

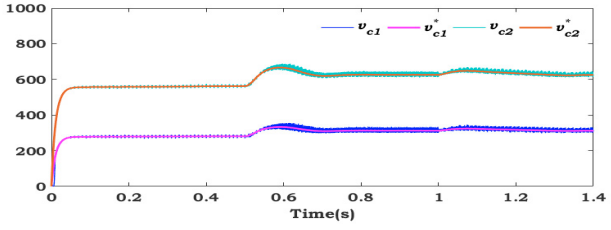

Fig. 5. Flying capacitor voltages

Table 3. THD in different operation modes

Mode	Total harmonic distortion THD (%)
Mode 1	2.44%
Mode 2	2.89%
Mode 3	1.10%

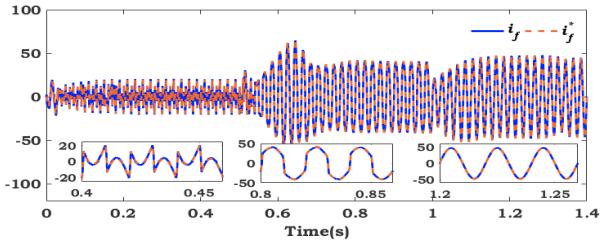

Fig. 6. Filter output current

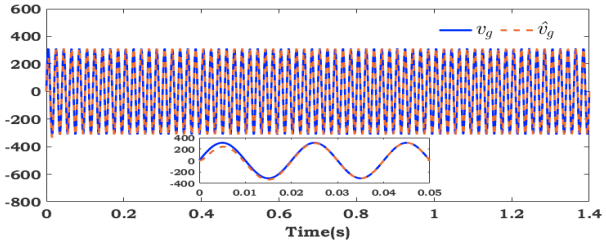

Fig. 7. Estimated grid voltage $\hat{x}_{2,g}$

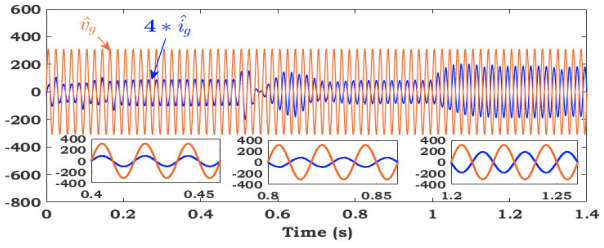

Fig. 8. Estimated grid current and voltage

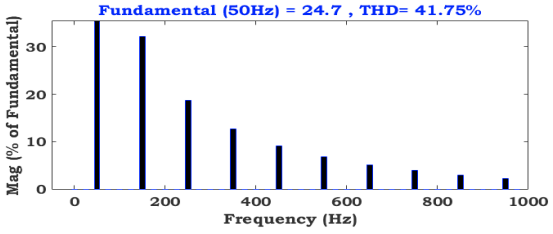

Fig. 9. FFT analysis of the load current

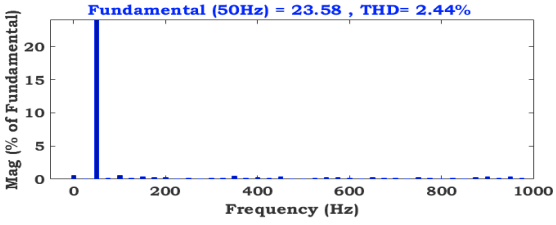

Fig. 10. FFT analysis of the power grid current

5. CONCLUSION

In this work, single stage grid connected PV system based on multicellular inverter with shunt active power filtering capability is investigated. From the obtained simulation results, it has been proved that the designed controller is able to extract the maximum power from PV generators and inject it into the power grid, as well as compensate harmonic currents and reactive power. As a result, a unity power factor is ensured which proved the effectiveness of the proposed controller. Besides, the FFT analysis of the grid current has demonstrated that a significantly lower THD was achieved, which is in compliance with the IEEE-519 standard.

REFERENCES

Abo-Elyousr, F.K. and Abdelaziz, A.Y. (2018). Optimal PI microcontroller-based realization for technical trends of single-stage single-phase grid-tied PV. *Engineering Science and Technology, an International Journal*, 21(5), 945–956.

Abouloifa, A., Giri, F., Lachkar, I., Chaoui, F.Z., Kissaoui, M., and Abouelmahjoub, Y. (2014). Cascade nonlinear control of shunt active power filters with average performance analysis. *Control Engineering Practice*, 26, 211–221.

Aouadi, C., Abouloifa, A., Lachkar, I., Hamdoun, A., Boussair, Y., Aourir, M., and Mchaour, Y. (2016). Multi loop based control of photovoltaic system connected to the single phase grid. In *2016 International Renewable and Sustainable Energy Conference (IRSEC)*, 479–483. IEEE.

Aourir, M., Abouloifa, A., Lachkar, I., Hamdoun, A., Giri, F., and Cuny, F. (2017). Nonlinear Control of PV System Connected to Single Phase Grid through Half Bridge Power Inverter. *IFAC-PapersOnLine*, 50(1), 741–746.

Jana, J., Saha, H., and Das Bhattacharya, K. (2017). A review of inverter topologies for single-phase grid-connected photovoltaic systems. *Renewable and Sustainable Energy Reviews*, 72, 1256–1270.

Karami, N., Moubayed, N., and Outbib, R. (2017). General review and classification of different MPPT Techniques. *Renewable and Sustainable Energy Reviews*, 68, 1–18.

Lada, M.Y., Mohamad, S.S., Gani, J.A.M., Nawawi, M.R.M., and Kim, G.C. (2016). Reduction of harmonic using single phase shunt active power filter based on instantaneous power theory for cascaded multilevel inverter. In *2016 IEEE International Conference on Power and Energy (PECon)*, 702–706. IEEE, Melaka, Malaysia.

Putri, R., Wibowo, S., and Rifa'i, M. (2015). Maximum Power Point Tracking for Photovoltaic Using Incremental Conductance Method. *Energy Procedia*, 68, 22–30.

Rodriguez, J., Bernet, S., Wu, B., Pontt, J.O., and Kouro, S. (2007). Multilevel Voltage-Source-Converter Topologies for Industrial Medium-Voltage Drives. *IEEE Trans. Ind. Electron.*, 54(6), 2930–2945.

Sefa, I., Altin, N., Ozdemir, S., and Kaplan, O. (2015). Fuzzy pi controlled inverter for grid interactive renewable energy systems. *IET Renewable Power Generation*, 9(7), 729–738.

Sinha Ray, A. and Bhattacharya, A. (2016). Improved tracking of shunt active power filter by sliding mode control. *International Journal of Electrical Power & Energy Systems*, 78, 916–925.